



Impact of Blood Rheological Strategies on the Optimization of Patient-Specific LAAO Configurations for Thrombus Assessment

Carlos Albers¹(✉), Andy L. Olivares¹, Xavier Iriart², Hubert Cochet²,
Jordi Mill¹, and Oscar Camara¹

¹ Sensing in Physiology and Biomedicine (PhySense), Department of Information and Communication Technologies, Universitat Pompeu Fabra, 08018 Barcelona, Spain
carlos.albers@upf.edu

² Hôpital Haut-Lévêque, Bordeaux, France

Abstract. Left atrial appendage occlusion devices (LAAO) are a feasible alternative for non-valvular atrial fibrillation (AF) patients at high risk of thromboembolic stroke and contraindication to antithrombotic therapies. However, optimal LAAO device configurations (i.e., size, type, location) remain unstandardized due to the large anatomical variability of the left atrial appendage (LAA) morphology, leading to a 4–6% incidence of device-related thrombus (DRT). In-silico simulations can be used to estimate the risk of DRT and identify the critical parameters, such as suboptimal device positioning. However, simulation outcomes depend a lot on a series of modelling assumptions such as blood behaviour. Therefore, in this work, we present fluid simulation results computed on two patient-specific LA geometries, using two different commercially available LAAO devices, located in two positions: 1) mimicking the real post-LAAO intervention configuration; and 2) an improved one better covering the pulmonary ridge for DRT prevention. Different blood modeling strategies were also tested. The results show flow recirculations at low velocities with significant platelet accumulation in LAA-deep device positioning uncovering the pulmonary ridge, potentially leading to thrombus formation. In addition, assuming Newtonian blood behaviour may result in an overestimation of DRT risk.

Keywords: Left atrial appendage occlusion · Blood behaviour · Platelet adhesion · Device related thrombus · In-silico fluid simulations

1 Introduction

Atrial fibrillation (AF) is a life-threatening condition with stroke prevention as a cornerstone of its clinical management. Among AF patients, >90% AF-related strokes develop in the ear-shaped and highly trabeculated cavity called the left atrial appendage (LAA) [4]. Although anticoagulation therapy is the first-line treatment, the non-negligible number (>50%) of non-valvular AF patients with

anticoagulants contraindications, along with the increasing incidence of the AF population, creates the unmet need to reduce the risk of stroke [9]. In the past decade, left atrial appendage occlusion (LAAO) has emanated with a potential role for stroke prevention. However, an effective LAAO device implantation requires a high level of expertise from clinicians, as the shape and size of the LAA can greatly vary. Therefore, device settings (e.g., design, size, position) must be accordingly tailored to avoid unusual events at follow-up such as device embolization, peri-device leaks, or device-related thrombus (DRT), due to sub-optimal device characteristics selection. Of these, thrombus formation on device surface, DRT, is the major concern of LAAO with a documented incidence of 4–6% [2]. The DRT mechanism appears to be a multifactorial process enrolling abnormal hemodynamic patterns related to the clinical patient characteristics (e.g., age, comorbidities), postoperative complications (e.g., incomplete device endothelialization, effusion), or deep-device-LAA implantation; recently correlated as a DRT-independent predictor [3, 5].

Transesophageal echocardiography (TEE) is the most commonly used imaging technique for LA/LAA morphological and hemodynamic (Doppler echocardiography) analysis, but the spatial and time resolution limitations may hinder the hemodynamic interpretations or measurements for device selection and consequently, DRT assessment. Cardiac computed tomography (CCT) modality or pre-planning tools (e.g., FEOPs HeartGuide [17], 3mensio [10], VIDAA platform [1]) can provide accurate morphological estimations and recommend better device settings, albeit disregarding the importance of blood flow patterns. Alternatively, in-silico flow simulations are an emerging powerful concept for the prevention of DRT that can help understand the morphology of LA/LAA and the complex characterization of blood flow. Multiple computational fluid dynamics (CFD) studies (see [15] for a recent literature review) have been published on the hemodynamics representation of the LA in patients with AF [6, 7, 14], including thrombus models with discrete phase methods (DPM) [23], and more recently, rheological characterization of blood with non-Newtonian approaches [8]. However, only a few investigations have incorporated the occlusion procedure. Some studies have focused on blood flow behavior in several device configurations [1]. Others have also added particles to mimic platelet adhesion to the surface of the device [19], and more advanced ones explore the mechanical properties of the devices for optimal in-silico representation of deployment [26].

Accordingly, the main goal of this work was to identify the impact of device configuration (type, size, position) in DRT risk post-LAAO intervention on two patient-specific geometries with DRT in follow-up scans with the resulting in-silico haemodynamic analysis. The most common commercialized devices (Amplatzer Amulet from Abbott Vascular, USA; and Watchman from Boston Scientific, USA) were virtually implanted in the real post-LAAO device settings and other proposed improved configurations for DRT prevention. Rheological blood variations and platelet concentrations were also tested.

2 Material and Methods

2.1 Clinical Data

Patient-specific 3D left atria geometries were extracted in Slicer 4.11¹ from the manually obtained binary mask segmentations of the retrospective pre- and post-occlusion computed tomography (CT) images provided by ANONYMOUS. The six-month follow-up CT scan showed the presence of a device-related thrombus in both of the cases analysed. Cardiac CT studies were performed on a 64-slice dual source CT system (Siemens Definition, Siemens Medical Systems, Forchheim, Germany) and then reconstructed into isotropic voxel sizes (0.37–0.5 mm range; $512 \times 512 \times [270\text{--}403]$ slices) after approval from the ethical committee and informed consent of the patient.

2.2 Occluder Device Configurations and 3D Model Generation

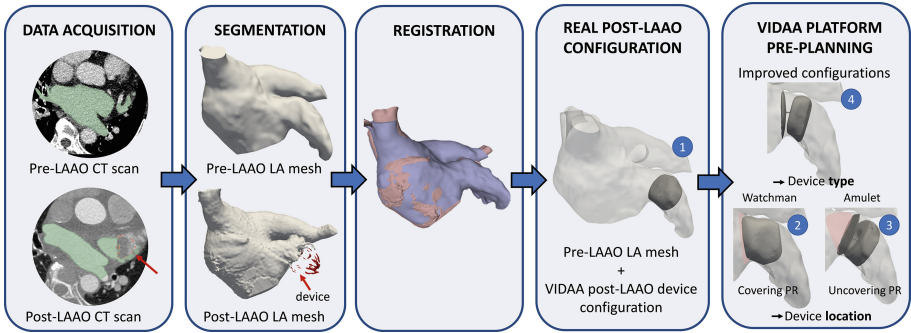


Fig. 1. Modeling pipeline of several device deployments in each of the patients. LAAO: Left atrial appendage occlusion; CT: computed tomography; PR:pulmonary ridge.

Two device positioning were defined for each patient. First, the real location of the LAAO device had to be extracted. To achieve that, apart from the pre- and post-CT LA geometries, the LAAO device was manually segmented in the post-CT images (Fig. 1 segmentation). Then, a fiducial registration from Meshlab v2021-07² was employed between pre- and post-LAAO meshes to place the CT segmented device in the pre-occlusion mesh (Fig. 1 registration). Finally, the segmented device and the pre-CT LA mesh were together uploaded into the web-based VIDAA platform [1] to simulate the device deployment with computer-aided design (CAD) models of the most used occluders; the plug type Watchman and the pacifier type Amplatzer Amulet. The device segmentation allows the identification of the device's size, type, and location from the post-CT images, which is then used for the selection of the CAD model of the device to deploy in

¹ <https://www.slicer.org/>.

² <http://www.meshlab.net>.

the pre-CT LA geometry. In both analysed patients, clinicians ended up implanting the devices quite deep in the LAA, i.e., uncovering the pulmonary ridge (lateral fold formed by the coalescence of the LAA and the Left Superior Pulmonary Vein (LSPV)); therefore, a second device positioning, closer to the ostium (interface between LA main cavity and the LAA) and covering the pulmonary ridge, was also evaluated. For this second configuration, the recommended LAAO device size was estimated within the VIDAA platform based on anatomical measurements following the guidelines provided by device manufacturers [13]. Both device designs (e.g., plug and pacifier devices) were implanted in each patient to test their performance. For Patient 1, both plug type device configurations (the real and the second proposed configuration) were mimicked with the pacifier type device. In Patient 2, the pacifier was the starting device. The result was four configurations per patient (see Fig. 1).

To solve the fluid domain, tetrahedral volumetric meshes of 12×10^5 elements were generated in Gmsh 4.8.4³ with the LAAO devices deployed and LA geometry downloaded from VIDAA. Mesh resolution follows the request proposed by [11], and sensitivities studies [15,20] in the field.

2.3 Computational Fluid Dynamic Simulations

Boundary Conditions and Setup of Simulations: Generic clinical measurements collected from a patient with AF were imposed to define the boundary conditions. Catheter pressure data and echo Doppler velocity profile were defined in the pulmonary veins and mitral valve, respectively, based on sensitivity analyses on LA-based fluid models [15]. Moreover, LA wall motion was included through a passive mitral valve annulus motion function from a half-scaled version of Veronesi et al. [21]. Then, a spring-based dynamic solution of the CFD solver was employed to ensure motion diffusion through the LA wall geometry. The model setup also included three boundary layers of 0.0001 mm thickness. Two cardiac cycles were simulated in 176 steps per beat with a time-step of 0.01 s, according to the patients heart rate (HR). In-silico studies were performed within the fluid flow solver Ansys Fluent 2022 (ANSYS Inc, USA).

Modelling Strategies for Rheological Variations: The different approaches to test the blood rheological scenarios were the following: i) the assumption of blood as a homogeneous and incompressible Newtonian fluid [6,16] with constant 1060 kg/m³ density and 0.0035 Pa·s viscosity; and ii) a Carreau model defining a non-Newtonian approach [7], where the viscosity is a function dependent on the shear rate. The dynamic viscosity behavior in Carreau's model is described by the following equation:

$$\eta = \eta_{\infty} + (\eta_0 - \eta_{\infty})[1 + \gamma^2 \lambda^2]^{(n-1)/2} \quad (1)$$

where λ as time constant, n the power-law index, η_0 the zero shear viscosity and η_{∞} , the infinite shear one. The values, $\mu_0 = 0.056$ Pa·s, $\mu_{\infty} = 0.0035$ Pa

³ <http://gmsh.info>.

Pa·s, $\lambda = 1.902$ s, $n = 0.3568$, were implemented from [25] to model the blood conditions.

Platelet Adhesion Model: Similar to Planas et al. [19], a first approximation of a thrombus model based on a discrete phase modeling (DPM) was combined with the continuous phase (blood flow). The DPM was coupled within the CFD solver to interact with the fluid flow and complement the DRT risk estimation. A given number of particles representing clusters of platelets were injected through the pulmonary veins during the initial 10 time steps of each beat of the cardiac cycles. The number of platelets per injection $n_{plat} = c_p \cdot V_{LA}$, particle diameter d_p , LA volume (V_{LA}), and total flow rate Q , were calculated accordingly for each patient. To do so, values such as particle density ($\rho_p = 1550$ kg m⁻³), molecular viscosity (μ_p), surface tension (σ_p), and blood platelet concentration ($c_p = 2 \cdot 10^8$ mL⁻¹) were assumed under physiological conditions⁴.

$$m_p \frac{d\mathbf{u}_p}{dt} = m_p \frac{\mathbf{u} - \mathbf{u}_p}{\tau_r} + \mathbf{F}, \quad (2)$$

where \mathbf{u} represents the fluid velocity, m_p the particle mass, \mathbf{u}_p the particle velocity, ρ the fluid density and the term $m_p (\mathbf{u} - \mathbf{u}_p) / \tau_r$, the drag force. The term, \mathbf{F} , describe the Saffman's lift force [12]. The inclusion of the DPM interaction in the CFD solver reported a slight difference in the LAA ostium average velocities in comparison to the cases only with the continuous domain solution. Nevertheless, due to the personalized characteristics of the particles, the influence of DPM on flow behavior was negligible. The platelets adhesion model defines the worst-case DRT scenario, in which all particles touching the LAA under certain conditions are adhered by the wall-film constraint imposed on the entire endothelial LAA wall. In platelets, the assumption of no division after their collision has been made, so there is no particle splashing. The O'Rourke [18] separation model with an angle of 90° is also taken into account. The number and location of platelets were used to estimate the risk of thrombus formation.

2.4 Hemodynamic Indices

Average velocities, the simulated blood flow patterns, and the endothelial cell activation potential (ECAP) were assessed on the device surface at key instants in the cardiac cycle. The δ viscosity metric ($\delta_{visc.} = nonNewt.visc. - Newt.visc.$) was incorporated to define the viscosity differences between non-Newtonian and Newtonian regimes. Additionally, the number of wall-adhered platelets was computed at the end of the simulation. All indices were calculated on the second cardiac beat to avoid convergence problems.

3 Results

The device configurations with the covered pulmonary ridge shown in Fig. 3 (third and fifth row) provided higher velocities without re-circulations patterns

⁴ <https://bionumbers.hms.harvard.edu/search.aspx>.

in the surrounding areas near the device surface. The presence of mean velocities below 0.2 m/s during atrial systole and sustained in diastole ($t = 0.6$ s) were only present in real LAAO positionings, which could indicate a higher risk of DRT, compared to the devices covering the PR. No significant differences were found between device types. However, the assumption of Newtonian models showed higher velocities compared to the non-Newtonian strategy (Fig. 3 black block).

High risk of coagulability is associated with the increase of number of wall-adhered platelets, commonly located in the pulmonary ridge region with deep-LAA positioning (Fig. 3 first, second and forth row). Moreover, susceptible areas with platelet accumulation were also seen in the plug type device even in the covered location due to the space left by the device surface curvature with the LAA endothelial wall. In contrast, the disk of the pacifier device allowed a better dispersion of the adhered platelets. Under the Newtonian regime, the highest deposition occurred in the plug device, with almost 20% of the platelets injected attached (Fig. 3 first row).

The ECAP maps in Fig. 3 (last column) display low values achieved for the pacifier device on both configurations (i.e., lowest risk of thrombus formation) due to the higher blood flow velocity values. Meanwhile, indistinctively of the location, the plug device obtained regions with ECAP values higher >1.5 , especially the uncovered location where the regions with the peak values matched the low velocities seen in the streamline calculation.

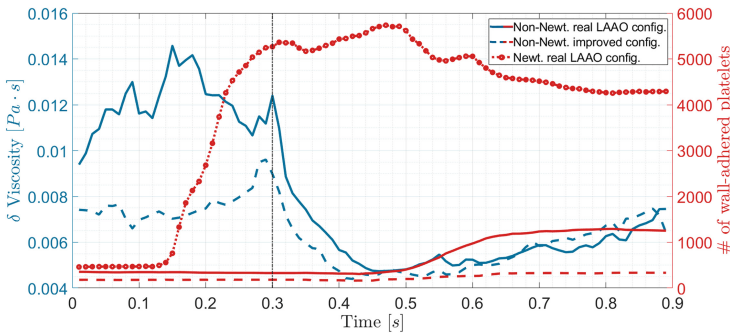


Fig. 2. Impact of viscosity changes on platelet accumulation near the device surface for real left atrial appendage (LAAO) occlusion and improved configuration covering the pulmonary ridge throughout the cardiac cycle with the different rheological strategies tested in Patient 1. Blue color represents the dynamic behavior of the δ viscosity (non-Newtonian viscosity - Newtonian viscosity) and the red color, the accumulation of platelets adhered to the wall. The gray line delimits the systolic ($t = 0-0.3$ s) and diastolic phases ($t = 0.31-0.65$ s). (Color figure online)

Finally, quantitative and temporal variations of blood viscosity in the device area can be seen in Fig. 2, showing higher viscosities in uncovered PR configurations within the LAA due to lower velocities than configurations proximal to

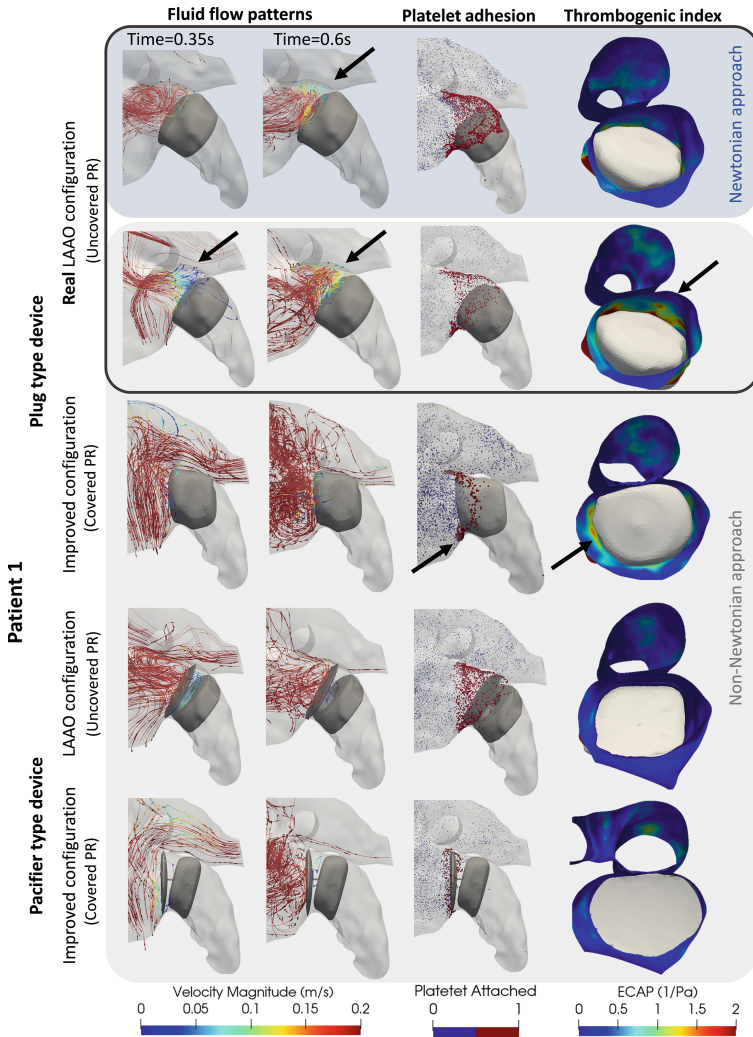


Fig. 3. Patient 1: The first two columns show the simulated blood flow patterns in the left atria (LA) in early- ($t = 0.35s$) and late- ($t = 0.6s$) diastole evaluated with various configurations of occluder devices. The third column corresponds to the platelet adhesion model at the end of the cardiac cycle ($t = 0.89s$) and, the last column represents the endothelial cell activation potential (ECAP) values of the endothelial wall of the appendage near the device surface by cutting at the level of the LAA ostium. A frontal view of the device's surface is shown in white. The black rectangle highlights the comparison between Newtonian and non-Newtonian models in the real LAAO configuration. The black arrows indicate re-circulation at low velocities, platelet accumulation, and high ECAP values on the device surface.

the location of the LAA ostium. In the non-Newtonian approach, the systolic phase displayed higher viscosities. Moreover, significant differences in platelet accumulation were evident in blood behavior models, with the Newtonian models exhibiting the highest platelet accumulation. Non-Newtonian models showed a rise in platelet accumulation coinciding with the E-wave in the diastolic phase, whereas Newtonian models exhibited an exponential increase prior to the opening of the mitral valve and a relatively maintained concentration throughout the cardiac cycle. Similar conclusions were obtained in Patient 2.

4 Discussion and Conclusions

The modeling of pathophysiological factors underlying thrombus formation with computational fluid simulations is not an easy endeavor. Moreover, the credibility of the in-silico models requires personalization and verification as a standardization process inside the V&V40 guidelines [22]. Hence, it is essential to compare models with different LA-based modeling choices to achieve best practices.

The clinical records of the patients analyzed reported a DRT post-intervention. A correct assessment and pathology interpretation requires a parameter combination following Virchow's triad [24]. In the present study, the primary drivers of blood stasis, hypercoagulability, and endothelial injury have been illustrated in a number of virtually implanted configurations that are not frequently reported in the literature. In addition, the virtual web-based platform VIDAA [1] has been employed to create different virtual occlusion configurations. The utilization of a platform such as VIDAA facilitates decision-making and leads to the attainment of an optimal configuration, thus minimizing instances of DRT. In our experiments, the deployment of all devices adhered to clinical standards and experimental data that lead to a satisfactory procedure.

Recent clinical studies [2] indicate a slightly better performance in DRT rates after intervention with the pacifier device compared to the plug, which is consistent with the hemodynamic results obtained from the simulation analysis. Lower velocities with re-circulations patterns were detected at the edges of the plug device, particularly in configurations where the device was positioned deeply. The performance of both devices improved when the pulmonary ridge was covered. This supports the conclusion of Freixa et al. [5] that such an approach may reduce the incidence of DRT. However, the presence of high ECAP values and some complex flow in the plug device even in the covered configuration suggest that device shape has a potential role in blood stasis. Moreover, a proximal location may not be always feasible, as it may lead to improper device compression or insufficient endothelization, rising the risk to suffer a mitral valve leaf's intersection (with the pacifier disk) or device embolization.

Previous studies in modeling fluid flow in atrial fibrillation (AF) have largely relied on the assumption of Newtonian rheology. However, Gonzalo et al. [8] recently discovered that this assumption led to an overestimation of the hypercoagulability state in AF patients. The current study concurs with these findings, revealing that variations in blood rheology significantly influence the platelet

adhesion model. The results indicate that there is a correlation between the amount of platelets adhered and increases in flow velocity, with this relationship being especially pronounced in the Newtonian approach (Fig. 2).

In the present study, the benefits of using real post-LAAO configurations in conjunction with non-Newtonian models for DRT stratification in fluid simulations were acknowledged. However, certain assumptions were made regarding the device placement (only the metallic structure was segmented in the plug device), CAD models, and the lack of patient-specific boundary conditions. To improve the realism of the models, further exploration is needed, such as incorporating shear stress in the platelet adhesion or using agent-based models.

Acknowledgement. This project has received funding from the European Union's Horizon 2020 research and innovation programme under grant agreement, No 101016496 (SimCardioTest).

References

1. Aguado, A.M., et al.: In silico optimization of left atrial appendage occluder implantation using interactive and modeling tools. *Front. Physiol.* **10**, 237 (2019)
2. Alkhouli, M., Ellis, C.R., Daniels, M., Coylewright, M., Nielsen-Kudsk, J.E., Holmes, D.R.: Left atrial appendage occlusion: current advances and remaining challenges. *JACC Adv.* 100136 (2022)
3. Aminian, A., et al.: Incidence, characterization, and clinical impact of device-related thrombus following left atrial appendage occlusion in the prospective global amplatzer amulet observational study. *JACC Cardiovasc. Interv.* **12**(11), 1003–1014 (2019)
4. Cresti, A., et al.: Prevalence of extra-appendage thrombosis in non-valvular atrial fibrillation and atrial flutter in patients undergoing cardioversion: a large transoesophageal echo study. *EuroIntervention* **15**(3), e225–e230 (2019)
5. Flores-Umanzor, E., et al.: Device related thrombosis after left atrial appendage occlusion: does thrombus location always predicts its origin? *J. Interv. Card. Electrophysiol.* **60**, 347–348 (2021)
6. García-Isla, G., et al.: Sensitivity analysis of geometrical parameters to study haemodynamics and thrombus formation in the left atrial appendage. *Int. J. Numer. Methods Biomed. Eng.* **34**(8), e3100 (2018)
7. García-Villalba, M., et al.: Demonstration of patient-specific simulations to assess left atrial appendage thrombogenesis risk. *Front. Physiol.* **12**, 596596 (2021)
8. Gonzalo, A., et al.: Non-newtonian blood rheology impacts left atrial stasis in patient-specific simulations. *Int. J. Numer. Methods Biomed. Eng.* e3597 (2022)
9. Holmes Jr, D.R., Alkhouli, M., Reddy, V.: Left atrial appendage occlusion for the unmet clinical needs of stroke prevention in nonvalvular atrial fibrillation. In: *Mayo Clinic Proceedings*, vol. 94, pp. 864–874. Elsevier (2019)
10. Imaging, P.M.: 3mensio Medical Imaging B.V. <https://www.3mensio.com/>
11. Khalili, E., Daversin-Catty, C., Olivares, A.L., Mill, J., Camara, O., Valen-Sendstad, K.: On the importance of fundamental computational fluid dynamics towards a robust and reliable model of left atrial flows: is there more than meets the eye? (2023). <https://arxiv.org/abs/2302.01716>
12. Li, A., Ahmadi, G.: Dispersion and deposition of spherical particles from point sources in a turbulent channel flow. *Aerosol Sci. Technol.* **16**(4), 209–226 (1992)

13. Lim, M.Y., Abou-Ismaïl, M.Y.: Left atrial appendage occlusion for management of atrial fibrillation in persons with hemophilia. *Thromb. Res.* **206**, 9–13 (2021)
14. Masci, A., et al.: A proof of concept for computational fluid dynamic analysis of the left atrium in atrial fibrillation on a patient-specific basis. *J. Biomech. Eng.* **142**(1) (2020)
15. Mill, J., et al.: Sensitivity analysis of in silico fluid simulations to predict thrombus formation after left atrial appendage occlusion. *Mathematics* **9**(18), 2304 (2021)
16. Mill, J., et al.: Impact of flow dynamics on device-related thrombosis after left atrial appendage occlusion. *Can. J. Cardiol.* **36**(6) (2020)
17. NV.F.: FEops HeartGuide. <https://feops.com/>
18. O'Rourke, P.J., Amsden, A.: A spray/wall interaction submodel for the kiva-3 wall film model. *SAE Trans.* 281–298 (2000)
19. Planas, E., et al.: In-silico analysis of device-related thrombosis for different left atrial appendage occluder settings. In: Puyol Antón, E., et al. (eds.) STACOM 2021. LNCS, vol. 13131, pp. 160–168. Springer, Cham (2022). https://doi.org/10.1007/978-3-030-93722-5_18
20. Pons, M.I., et al.: Joint analysis of morphological parameters and in silico haemodynamics of the left atrial appendage for thrombogenic risk assessment. *J. Interv. Cardiol.* **2022** (2022)
21. Veronesi, F., et al.: Quantification of mitral apparatus dynamics in functional and ischemic mitral regurgitation using real-time 3-dimensional echocardiography. *J. Am. Soc. Echocardiogr.* **21**(4), 347–354 (2008)
22. Viceconti, M., Pappalardo, F., Rodriguez, B., Horner, M., Bischoff, J., Tshinanu, F.M.: In silico trials: Verification, validation and uncertainty quantification of predictive models used in the regulatory evaluation of biomedical products. *Methods* **185**, 120–127 (2021)
23. Wang, Y., Qiao, Y., Mao, Y., Jiang, C., Fan, J., Luo, K.: Numerical prediction of thrombosis risk in left atrium under atrial fibrillation. *Math. Biosci. Eng.* **17**(3), 2348–2360 (2020)
24. Watson, T., Shantsila, E., Lip, G.Y.: Mechanisms of thrombogenesis in atrial fibrillation: Virchow's triad revisited. *Lancet* **373**(9658), 155–166 (2009)
25. Weddell, J.C., Kwack, J., Imoukhuede, P., Masud, A.: Hemodynamic analysis in an idealized artery tree: differences in wall shear stress between newtonian and non-newtonian blood models. *PLoS ONE* **10**(4), e0124575 (2015)
26. Zaccaria, A., et al.: Left atrial appendage occlusion device: development and validation of a finite element model. *Med. Eng. Phys.* **82**, 104–118 (2020)